Full length Article

Structure of fungal communities in sequencing batch reactors operated at different salinities for the selection of triacylglyceride-producers from a fish-canning lipid-rich waste stream

David Correa-Galeote [a,b,*], Lucía Argiz [c], Anuska Mosquera-Corral [c], Angeles Val del Rio [c], Belen Juarez-Jimenez [a,b], Jesús Gonzalez-Lopez [a,b], Belen Rodelas [a,b]

[a] *Microbiology Department, Faculty of Pharmacy, University of Granada, 18001 Granada, Andalucía, Spain*
[b] *Microbiology and Environmental technology section, Microbiology Department, Faculty of Pharmacy, University of Granada, 18011 Granada, Andalucía, Spain*
[c] *CRETUS Institute, Department of Chemical Engineering, University of Santiago de Compostela, 15782 Santiago de Compostela, Galicia, Spain*

ARTICLE INFO

ABSTRACT

Oleaginous fungi natively accumulate large amounts of triacylglycerides (TAG), widely used as precursors for sustainable biodiesel production. However, little attention has been paid to the diversity and roles of fungal mixed microbial cultures (MMCs) in sequencing batch reactors (SBR). In this study, a lipid-rich stream produced in the fish-canning industry was used as a substrate in two laboratory-scale SBRs operated under the feast/famine (F/F) regime to enrich microorganisms with high TAG-storage ability, under two different concentrations of NaCl (SBR-N: 0.5 g/L; SBR-S: 10 g/L). The size of the fungal community in the enriched activated sludge (EAS) was analyzed using 18S rRNA-based qPCR, and the fungal community structure was determined by Illumina sequencing. The different selective pressures (feeding strategy and control of pH) implemented in the enrichment SBRs throughout operation increased the abundance of total fungi. In general, there was an enrichment of genera previously identified as TAG-accumulating fungi (*Apiotrichum*, *Candida*, *Cutaneotrichosporon*, *Geotrichum*, *Haglerozyma*, *Metarhizium*, *Mortierella*, *Saccharomycopsis*, and *Yarrowia*) in both SBRs. However, the observed increase of their relative abundances throughout operation was not significantly linked to a higher TAG accumulation.

1. Introduction

Population growth and lifestyle changes have led to higher energy requirements resulting in a worldwide interest in pursuing novel and renewable energy sources [1]. In this regard, biodiesel is one of the most promising sustainable and renewable substitutes for fossil diesel fuel [2] and is also a substitute for petroleum diesel as feedstock for the synthesis of chemicals and the manufacture of plastics [3].

The key features of the sustainability and environmental friendliness of biodiesel are based on its reduced CO_2 emission levels without sulphur and aromatic content (reviewed in [2]). Biodiesel is composed of a mixture of fatty acid alkyl esters produced by trans-esterification of triacylglycerides (TAG) with short-chain alcohols [4]. Originally, TAG

production was mainly restricted to the use of edible plant oils (mostly soybean, canola, or rapeseed), which limited biodiesel production feasibility due to the high production costs associated with, and the use of, food and feed commodities [2]. Therefore, different research attempts have been encouraged towards the utilization of lipid-rich wastes as biodiesel precursors. One of the most promising alternatives is the use of oleaginous microorganisms (bacteria, filamentous fungi, yeast, and microalgae) able to accumulate lipids intracellularly to > 20 % of their dry weight, assimilating different organic sources when they are subjected to an excess of carbon source under the limitation of other nutrients [4].

Fungi are considered the most promising microorganisms for the production of lipids useful in generating biofuels. Oleaginous fungi have

numerous advantages over other microbes, such as higher accumulation rates, greater tolerance to metal ions, larger cell size and easier harvesting than microalgae and bacteria [4]. Currently, only 30 different fungal genera and over 50 species have been described as oleaginous [5], and the lipid accumulating capacity is distributed throughout *Ascomycota, Basidiomycota,* and *Mucoromycota* [5,6]. Fungi use either hydrophilic or hydrophobic substrates as carbon sources for lipid synthesis, via *de novo* or *ex novo* pathways, respectively. Whereas the *de novo* pathway requires the limitation of key nutrients other than carbon, mainly nitrogen [7], the *ex novo* pathway is independent of the nitrogen exhaustion of the culture medium [8]. Regardless of the pathway followed for the conversion of the carbon substrates into fatty acids, TAG biosynthesis occurs mainly through the Kennedy pathway (reviewed by [4] and [9]). The enzymatic reaction considered as the limiting step for TAG biosynthesis is the dephosphorylation of phosphatidic acid to produce diacylglycerol [10]. The use of hydrophilic substrates through the *de novo* pathway is characterized in several fungal genera, while only a few (i.e., *Yarrowia, Cryptococcus, Rhodosporidium, Geotrichum,* and *Trichosporon*) accumulate lipids from hydrophobic substrates such as waste fish oil via the *ex novo* pathway [8].

Although oleaginous microorganisms constitute an alternative with great potential, especially in terms of productivity [4], the use of expensive carbon sources and pure microbial cultures increases production costs, making it less attractive and less competitive [11]. In this regard, research is now focused on the use of low-cost materials for TAG production, such as the cheap waste streams generated in several agri-food facilities [12] or fish-canneries [13]. This, along with the use of open mixed microbial cultures (MMCs) enriched in TAG-storing-populations, will notably increase the process economic feasibility [14]. This strategy is also more advantageous than generating biodiesel directly from lipid-rich wastes, which often have a high content of free fatty acids that, if not removed by pre-treatment (ideally to a value < 0.5 %), generate unwanted soaps during homogeneous alkaline catalyzed transesterification and hamper the purification of biodiesel [15]. In contrast, microbial biomass can be subjected to in situ lipid extraction and transesterification to generate biodiesel in a single step, reducing the total cost by eliminating the extraction and refining processes [16]. In addition, TAGs from oleaginous fungi have a fatty acid composition similar to that of vegetable oils, mainly consisting of C16 to C18 fatty acids, which are favorable for biodiesel production [17].

The new biotechnological "omic" tools have accelerated the acquisition of knowledge of complex microbial communities in different ecosystems [18,19]. Nevertheless, little attention has been paid to the microbial diversity of MMCs as cost-effective producers of TAG from oily wastes. Moreover, understanding of the relationships between the operating conditions and the development of the fungal lipid-accumulating communities is limited.

Recently, the possibility of valorizing a residual fish-canning oily stream into TAG in lab-scale open systems, under a feast/famine (F/F) selection strategy was demonstrated [20,21]. Since salinity was previously reported as a major factor influencing the fungal metabolism [22] and the structure of the eukaryotic communities in the activated sludge of fish-canning wastewater treatment plants (WWTPs) [18], two bioreactors were operated under different concentrations of NaCl (0.5 or 10 g/L), which fall within the range often found in fish-canning factory effluents [18]. The present study aimed to investigate the abundance and diversity of fungal populations in the MMCs enriched in TAG-accumulating fungi, using qPCR and high-throughput Illumina Miseq sequencing, respectively. Links between the biotic data, the operational variables, and the TAG-accumulation efficiencies were explored.

2. Material and methods

2.1. Bioreactor set-up and operation for the enrichment of TAG-accumulating biomass

Two laboratory-scale (4 L) sequencing batch reactors (SBR) were operated under the feast/famine (F/F) regime, under two different concentrations of NaCl (SBR-N, 0.5 g/L, and SBR-S, 10 g/L). A residual oily stream from the fish-canning industry (see details in Supplementary Table SI1) was used as the substrate. SBR-N was inoculated with activated sludge (AS) from an urban WWTP, whereas SBR-S was inoculated with AS from an industrial WWTP treating saline fish-canning effluents (10 – 15 g NaCl/L), in order to avoid a very long start-up period by using a microbial community already adapted to the selected salinity level. Both SBRs were operated in 12 h cycles, exchanging half of their volumes (2 L) at the end resulting in hydraulic and solid retention times of 24 h. At the beginning of each cycle, 114.5 Cmmol of substrate were added. Also, 2 L of dilution water (Supplementary Table SI2) were supplied to each SBR at different times, depending on the feeding strategy. The SBRs were continuously aerated, the temperature was maintained at 30 ± 3 °C, and the pH was controlled off-line by NaHCO$_3$ addition. Full details concerning operation of the reactors were as previously described [20,21].

SBR-N and SBR-S were operated for 331 and 122 days. Both operations were subdivided into start-up (NS and SS, for SBR-N and SBR-S, respectively) plus three analogous operational periods (NI, NII, NIII for SBR-N, and SI, SII, SIII for SBR-S). These were defined by two nitrogen-feeding strategies (periods NI and SI vs. NII and SII), and pH conditions during the famine phase (periods NII and SII (average pH 6.67 and 7.01, respectively) vs. NIII and SIII (average pH 5.70 and 6.59, respectively)). The operational cycles run in each period and periods' length are detailed in Supplementary Figure SI1.

2.2. Analytical methods and calculations

The pH was monitored by a pH and Ion meter (GLP22, Crison, Spain). Total and volatile suspended solids (TSS and VSS, respectively) were measured according to APHA [23]. Ions were determined by ion chromatography (861 Advanced Compact IC, Metrohm, Herisau, Switzerland), and total nitrogen (TN) was measured by catalytic combustion (TOC-L analyzer with the TNM- module, TOC-5000 Shimadzu, Kyoto, Japan). Analyses in the soluble fraction (ions and TN) were performed in centrifuged (Centrifuge 5430, Eppendorf, Hamburg, Germany) and filtered raw samples (0.45 μm pore size, cellulose-ester membrane, Advantec, Tokyo, Japan).

TAGs were identified and quantified in the lyophilized biomass samples by gas chromatography (HP innovax column equipped with a flame injection detector (FID), Agilent, Santa Clara, CA, USA) following the procedure described by [24]. Commercial calibration standards of palmitic-, stearic-, oleic-, and linoleic- acids were used (Sigma Aldrich, St Louis, MO, USA).

2.3. DNA extraction and purification

Enriched activated sludge (EAS) samples (9–332 mL) were periodically collected and subsample aliquots were immediately stored at −20 °C. DNA was isolated simultaneously from all the biomass samples using the FastDNA-2 mL SPIN Kit for Soil and the FastPrep24 apparatus (MP-BIO, Santa Ana, CA, USA), according to [18,19]. Two independent biological replicates were used from each sampling time. DNAs were stored at −20 °C until further use.

2.4. Quantitative polymerase chain reaction (qPCR)

Quantification of total fungi was performed using a quantitative PCR (qPCR) approach targeting the fungal 18S rRNA gene on a QuantStudio-

3 Real-Time PCR system (Applied Biosystems, Waltham, MA, USA) using the primers FungiQuantF (5′-GGRAAACTCACCAGGTCCAG-3′) and FungiQuantR (5′-GSWCTATCCCCAKCACGA) [25]. Reaction mixtures and cycling conditions are described in [18,26]. Each biological sample was tested in triplicate in two independent experiments.

2.5. Fungal 18S rRNA gene amplicon sequencing and bioinformatics workflow

Amplification (two independent replicates per sampling) of the hypervariable V5-V7 region of the 18S rRNA gene was performed using the same primers as for the qPCR analysis. Raw data from Illumina MiSeq sequencing were processed using the software Mothur v1.44.1 [27] according to the MothurMiSeq guidelines (https://mothur.org/wiki/miseq_sop/). Paired-end reads combination, primer trimming, quality filtering, identification of unique sequences, and chimeric analyses were made according to [18,19]. The resulting sequences were *de novo* clustered into OTUs (97 % similarity threshold), and only those with an abundance > 8 sequences (relative abundance (RA) > 0.0001 %) in the whole data set were considered for later diversity analysis. Finally, the consensus sequences of each OTU was taxonomically classified through the blast suite of the Geneious 2021.1.1 software (Biomatters, Auckland, New Zealand) against the fungal 18S rRNA NCBI database (www.ftp.ncbi.nlm.nih.gov/blast/db/). Nucleotide sequences were deposited in GenBank (accession number SUB9070410). The rarefaction curves were made using the iNEXT software (http://chao.stat.nthu.edu.tw/wordpress/software_download/inext-online/). Simpson and Shannon biodiversity indexes were calculated according to [28].

2.6. Statistical analysis

The non-parametric Mann-Whitney and Kruskal-Wallis (Conover-Iman pairwise test) tests were used to explore statistical differences ($p < 0.05$ significance level) among the corresponding samples using the XLSTAT v2021.1.1 software (Addinsoft, Paris, France). A nonmetric multidimensional scaling (NMS) analysis was driven using the PC-ORD software (Wild Blueberry Media, Corvallis, OR, USA). Correlations among the relative abundances (RAs) of the main fungal genera (those with a mean RA > 0.5 %) were calculated using Spearman's rank correlation coefficients in XLSTAT. Correlations were considered robust if the absolute value of the coefficient was > 0.7 ($p < 0.05$), and a co-occurrence network was constructed using the Fruchterman Reingold algorithm in the Gephi v0.9.2 software (Gephi Consortium, Paris, France). Finally, a heatmap of the RAs of the main fungal genera was constructed using the ward.D method in the R studio v.3.4.1 package (Rstudio, Boston, MA, USA).

3. Results and discussion

3.1. Summary of operating strategy and TAG accumulation efficiency in the SRBs

During the start-up and the first operational period in both SBRs (NS, SS, NI, and SI), carbon and nitrogen sources were added together at the beginning of each cycle (conventional aerobic dynamic feeding, ADF). Once the steady-state was reached, mean TAG-accumulations were 15.70 and 12.37 wt% in SBR-N and SBR-S, respectively. In periods NII and SII, the addition of carbon and nitrogen sources was uncoupled, and nitrogen availability was limited during the feast phase to evaluate the effect of the double growth limitation (DGL) enrichment strategy. As a result, TAG accumulation was sharply reduced compared to periods NI and SI (7.99 % wt and 3.36 % wt, NII and SII, respectively). Finally, since many fungi exhibit optimal growth at pH ranging 4–6 [22], the DGL strategy was combined during periods NIII and SIII with a reduction of NaHCO₃ supply, to evaluate its effect on the fungal community structure and TAG accumulation yields. This resulted in a reduction of pH in NIII

(5.70 in NIII vs. 6.67 in NII), which restored the TAG-storage capacity in SBR-N to the level achieved in period NI (16.82 wt% in NIII). However, not enough acidification was achieved in SBR-S (7.01 vs. 6.50 in SII and SIII, respectively), hampering TAG-accumulation capacity (2.10 wt% in SIII) [20,21].

3.2. Abundance of fungal populations in the MMCs

3.2.1. Quantification of 18S rRNA gene copies by qPCR

The fungal 18S rRNA gene copy numbers varied from a non-detectable level ($< 1.00 \times 10^5$ gene copies/L of EAS) to 4.10×10^{11} gene copies/L of EAS (Fig. 1). Accordingly, there were high variances in the absolute abundances of fungi regardless of the NaCl concentration or the source of inoculum. As this appears to be the first study to quantify the fungal populations using a qPCR approach in enriched MMCs of TAG-storing SBRs operated under the F/F regime, comparison with similar processes cannot be provided. However, the numbers of fungal 18S rRNA gene copies/L of EAS fell within the range previously described in conventional AS systems treating municipal or industrial wastewaters (WW) [18,19,26,29].

3.2.2. Effects of the operating conditions on the absolute abundance of fungi

According to Fig. 1, there were statistical differences in the absolute abundances of fungal populations in the SBRs among the different operational periods. Higher abundances were found after the implementation of the DGL strategy in the NII, SII, NIII and SIII periods. Lower numbers of 18S rRNA gene copies were found during periods NS, SS, NI and SI, without statistical differences either between periods NS and NI or between periods SS and SI. Thus, uncoupling the addition of carbon and nitrogen sources consistently increased the total abundance of fungi in both SBRs, a result in agreement with that previously found in an aerobic granular sludge SBR treating agricultural WW by applying microscopic techniques [30].

Regarding the comparison between the two bioreactors, statistically significant differences were also observed. During the start-up, the highest average numbers were found in period SS compared to NS (3.13×10^8 and 2.46×10^8 gene copies/L EAS, respectively). However, by the end of the experiment, the highest counts were observed in the SBR-N (3.56×10^{10} and 2.36×10^9 gene copies/L EAS for periods NIII and SIII, respectively). No significant differences were observed between NI and SI, or NII and SII (Fig. 1).

3.3. Fungal community structure and diversity

3.3.1. OTU richness and biodiversity

The number of high-quality fungal sequences was 7,055,143 (average 76,686 sequences per library) and the total number of OTUs was 376 (average 45 OTUs per library). The OTU abundance distribution and classification are shown in Supplementary Table SI3. The rarefaction curves are displayed in Supplementary Figure SI2. For SBR-N, the highest number of OTUs and Shannon index values were found in the NS (Supplementary Table SI4), with no statistical differences for the other three periods. Simpson index values were higher for the samples taken during periods NI, NII and NIII, and lower during NS. On the other hand, the number of OTUs and Shannon index values found in the samples from the SS and SI periods were higher than those observed during the SII and SIII periods. Reciprocally, the Simpson index values were statistically lower for the samples taken in SS and SI, and higher during SII and SIII. Thus, the richness and evenness of the fungal community did not register drastic changes after reaching the steady-state in SBR-N, while the DGL enrichment strategy induced a major transformation of the fungal community in SBR-S. Regarding statistical differences in the biodiversity between reactors for a given period, the OTU richness values in the NS and NII periods were higher than those found in SS and SII, respectively, while no significant differences were
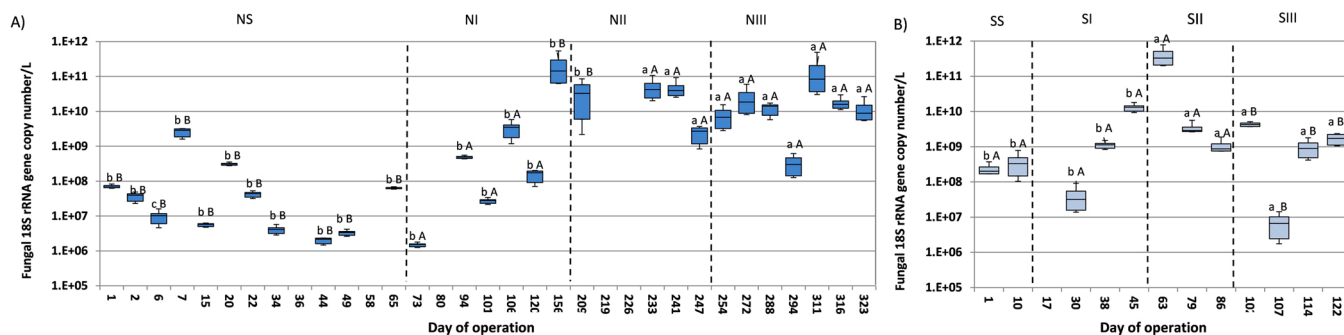
Fig. 1. Gene copies of fungal 18S rRNA per L of EAS determined by quantitative PCR in sludge samples (n = 2) retrieved from enrichment SBRs operated under two concentrations of NaCl (SBR-N: 0.5 g/L; SBR-S: 10 g/L). Lower case letters indicate significant differences among periods for a given reactor according to the Kruskal-Wallis and Conover-Iman tests (*p* < 0.05). Capital letters indicate significant differences between reactors for a given period according to the Mann-Whitney test (*p* < 0.05).

observed among periods NI and SI or NIII and SIII. Hence, despite the differences in the origin of the inoculum and the NaCl concentration, the operating conditions implemented in both reactors strongly shaped the richness and evenness of the fungal communities, which were similar to those observed in SBRs treating swine [31] and urban WW [32].

3.3.2. Fungal community structure at the phylum level

Out of 376 different OTUs, a total of 353 (7,040,705 sequences) belonged to 8 different fungal phyla plus a group of *Dikarya* sequences not classified at the phylum level. 23 OTUs (14,438 sequences) were not classified within the fungal domain and were removed from the analysis. The RAs of the dominant phyla (RA > 0.1 %) are displayed in Fig. 2 and Table SI5. Sorted in decreasing order of average RA they were: *Ascomycota* (48.24 %), *Basidiomycota* (37.00 %), *Chytridiomycota* (7.39 %), *Mucoromycota* (7.03 %), the grouped minority phyla (0.12 %) and unclassified fungal sequences (0.24 %). The RA of non-classified fungal OTUs was lower than previously found in other studies that analyzed the operation of SBRs [31,32].

In general, the fungal community structure at the phylum level was in agreement with the previously described in WWTPs, including several full-scale facilities [33–35], and in lipid-accumulating fed-batch cultures [36].

3.3.3. Fungal community structure at the genus level

The 376 OTUs were distributed into 142 different genera plus the unclassified sequences group. 20 genera displayed RAs > 0.5 % and were considered the main dominant genera. Their distribution among the samples is shown in Fig. 3 and Supplementary Table SI6. These main dominant genera were, sorted in decreasing RA order: *Apiotrichum* (31.24 %), *Geotrichum* (20.61 %), *Candida* (15.98 %), *Mortierella* (6.44 %), *Pendulichytrium* (6.05 %), *Cutaneotrichosporon* (1.73 %), *Yarrowia* (1.61 %), *Fonsecaea* (1.55 %), *Zasmidium* (1.31 %), *Hyaloraphidium*

(1.29 %), *Wickerhamiella* (1.21 %), *Schizonella* (1.04 %), *Metarhizium* (0.91 %), *Malassezia* (0.85 %), *Jimgerdemannia* (0.75 %), *Clydaea* (0.71 %), *Classicula* (0.66 %), *Haglerozyma* (0.61 %), *Vinositunica* (0.59 %), and *Saccharomycopsis* (0.55 %).

Altogether, these 20 dominant genera represented more than 95 % (average 94.40 % per library) of the total fungal sequences, except in the samples taken at the beginning of the NS and SS periods, in which they only accounted for 82 % and 32 %, respectively. Some of the aforementioned genera, mainly *Apiotrichum*, *Candida*, *Cutaneotrichosporon*, *Geotrichum*, *Fonsecaea*, *Malassezia*, *Mortierella*, *Wickerhamiella* and *Yarrowia* have been found previously as well as dominant members of fungal communities in WWTPs based on different technologies [18,31, 35–40]. The remaining dominant genera have not been previously described as main members in any type of WWTP.

Also, it is worth noting that the fungal core of the two SBRs was restricted to only two dominant genera, *Apiotrichum* and *Candida*, whose cumulative RAs amounted to nearly half of the total fungal community. Additionally, the different SBR-N samples also shared *Cutaneotrichosporon*, *Geotrichum*, *Hyaloraphidium*, and *Mortierella*, whereas *Malassezia*, *Wickerhamomyces* and *Zasmidium* were exclusively shared by samples taken from SBR-S. Thus, a low degree of synchrony at the genus level was found, in agreement with the results reported previously [18], where it was found that the fungal core of 4 different fish-canning WWTPs comprised only 3 of the 82 genera described there. The cumulative RA of the shared genera in each bioreactor was close to 80 % (77.41 % and 83.20 % in SBR-N and SBR-S, respectively), and thus they constituted most of the fungal communities.

The co-occurrence networks of each bioreactor are illustrated in Fig. 4a, b. The resulting network of SBR-N consisted of 21 nodes and 142 edges (88 positives and 54 negatives), representing 34 % of the potential correlations. Similarly, in the SBR-S, the network was composed of 18 nodes and 96 edges (60 positives and 36 negatives), which corresponded
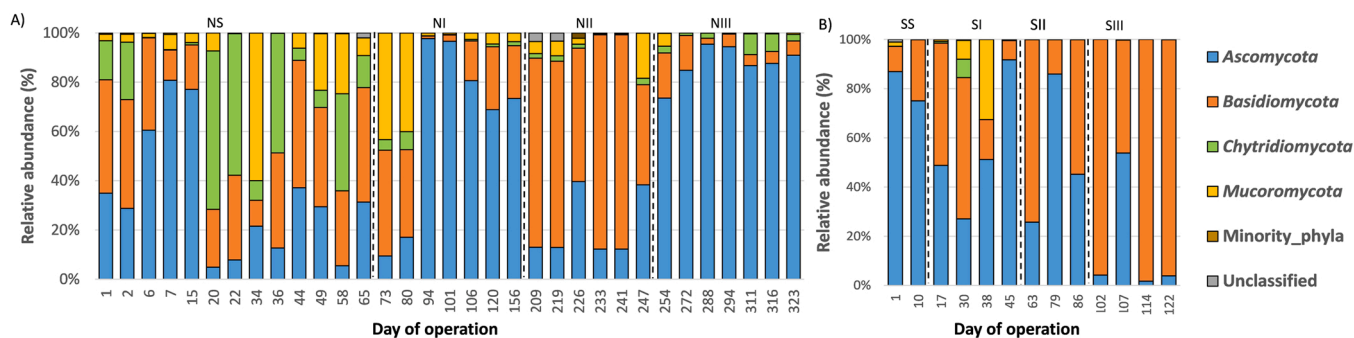

Fig. 2. Average relative abundance of dominant fungal phyla (RA > 0.1 %) identified by high-throughput Illumina sequencing in EAS (n = 2) from enrichment SBRs operated under two concentrations of NaCl: (A) 0.5 g/L NaCl (SBR-N) and (B) 10 g NaCl/L (SBR-S).
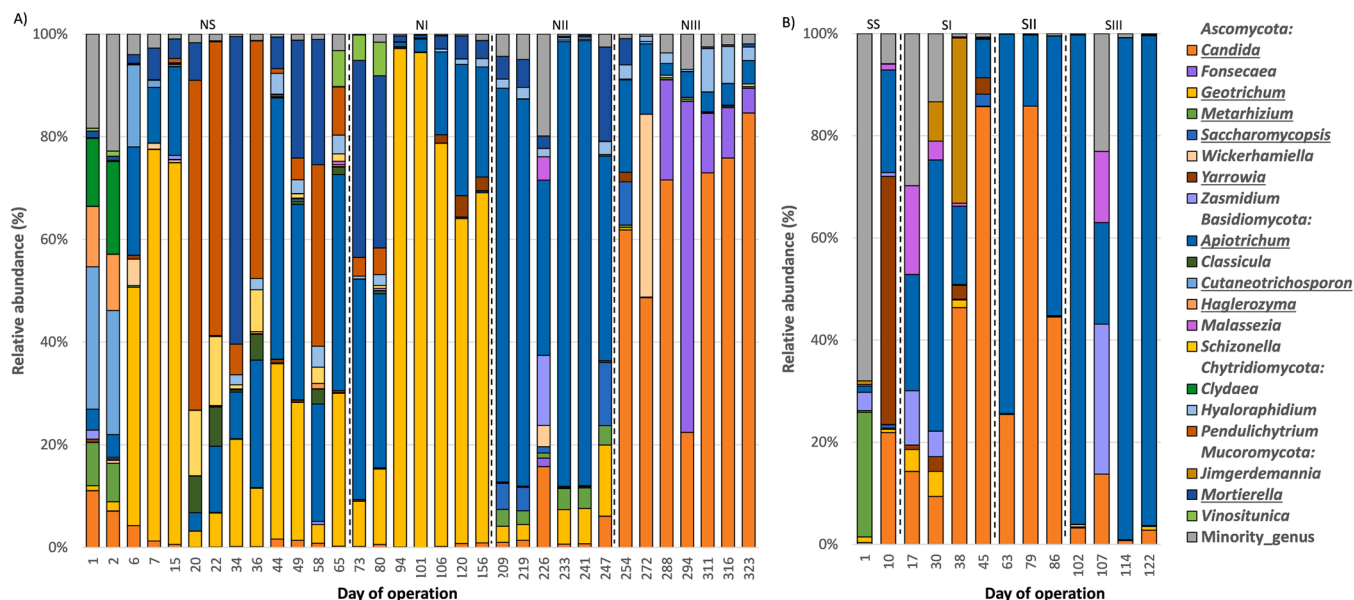
Fig. 3. Average relative abundance of dominant fungal genera (RA > 0.5 %) identified by high-throughput Illumina sequencing in EAS (n = 2) from enrichment SBRs operated under two concentrations of NaCl: (A) 0.5 g/L (SBR-N) and (B) 10 g/L (SBR-S). The genera underlined have been previously described as TAG accumulators.
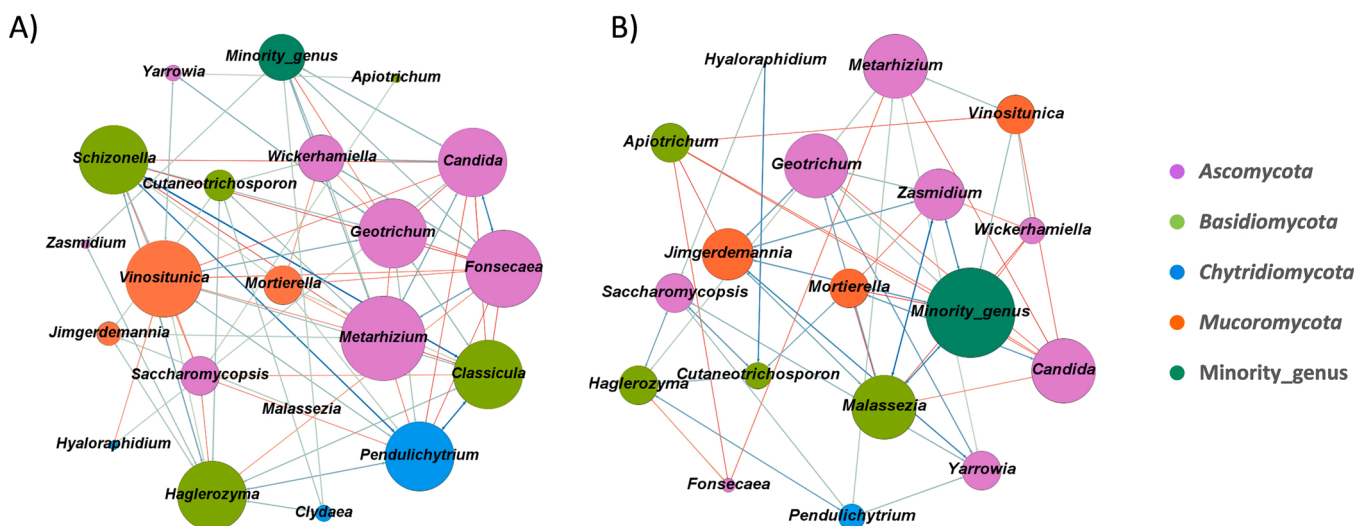

Fig. 4. Co-occurrence network of dominant fungal genera (RA > 0.5 %) sequencing in EAS (n = 2) from SBRs operated under two concentrations of NaCl (SBR-N: 0.5 g/L (A); SBR-S: 10 g/L (B)) using the Fruchterman Reingold algorithm. Size of each node is proportional to the number of interactions; blue and red edges correspond to positive and negative Spearman's correlation coefficients, respectively.

to 32 % of the total possible correlations. Hence, similar levels of complexity were observed between the two SBRs with a predominance of synergistic interrelationships between fungal genera.

The composition of nodes and edges differed within each network and, consequently, a different co-occurrence topology among both reactors was found. The genera acting as hubs in SBR-N were *Candida, Classicula, Fonsecaea, Geotrichum, Haglerozyma, Metarhizium, Schizonella,* and *Vinositunica,* while those more densely interconnected in SBR-S were *Candida, Geotrichum, Jimgerdemannia, Malassezia, Metarhizium, Zasmidium,* and the group of minority genera. *Metarhizium, Geotrichum,* and *Candida* acted as keystones in the two reactors, highlighting their importance in the enriched TAG-accumulating community, according to their high potential for extensive cooperation and syntrophic interactions in both reactors [41]. It is important to note that *Candida,* with a well-known TAG-accumulating capacity as will be further discussed, was identified as a core genus in both bioreactors. The presence

of *Candida* in different types of WWTPs has been described earlier [42]. *Candida* can degrade several pollutants (phenol, n-alkylbenzenes, n-alkanes), metabolize crude oils [42], and can synthesize extracellular polymers beneficial for the bioreactor performance [43]. Therefore, *Candida* is a promising tool in TAG synthesis and storage in SBRs, that can also play essential roles in maintaining the network structure under the two NaCl concentrations tested.

3.4. Influence of the operating conditions on the fungal community structure

Statistically significant differences in the RAs of the dominant fungal phyla were found when comparing either between the operational periods in the same SBR, or between the two SBRs in the same operational period (Supplementary Table SI5). In the SBR-N, the RAs of *Ascomycota* were significantly higher at the end of the experiment (NIII), while in the

SBR-S the RA of this phylum was the lowest in period SIII. In contrast, *Basidiomycota* reached their significantly lowest RAs in periods NIII and SS. The RA of *Chytridiomycota* was significantly higher in the samples taken during the NS period compared to NI, NII and NIII, while in the SBR-S, members of this phylum were only detected in low RA (average 2.06 %) during period SI. The RAs of *Mucoromycota* were significantly reduced in both SBRs by the end of the experiment (periods NIII and SIII). These results show that the implementation of the same enrichment strategies did not result in similar modifications of the fungal community assembly in both reactors.

The heatmap of the RAs of the dominant fungal genera (Supplementary Figure SI3) shows that for each sample, there were prevalent populations with higher than average RAs. In agreement with the results described at the phylum level, there were significant differences in the RAs of the dominant fungal genera among the four operational periods in each SBR (Supplementary Table SI6). Some of these major genera were only detectable in one of the SBRs: *Classicula*, *Clydaea*, *Haglerozyma*, *Pendulichytrium* and *Schizonella* were exclusively in SBR-N, and *Jimgerdemannia* was exclusively in SBR-S. Throughout the four experimental periods, no significant differences were found among the RAs of *Malassezia* and *Zasmidium* in any of the SBRs, or among those of *Cutaneotrichosporon*, *Fonsecaea*, *Hyaloraphidium*, *Mortierella*, *Saccharomycopsis*, *Vinositunica*, and *Wickerhamiella* in the SBR-S.

Three genera alternated as the dominant members of the fungal community in the SBR-N (Supplementary Table SI6). *Geotrichum* (25.88

%) and *Apiotrichum* (20.16 %) codominated in the NS period, and although *Geotrichum* increased its average RA up to 61 % in NI, it was replaced by *Apiotrichum* as the major genus in NII (66.57 %), after the DGL strategy was implemented. Subsequently, when NaCO$_3$ addition was reduced (average pH 5.70), *Candida* increased its average RA 15-fold from NII to NIII, concomitantly with a 9-fold reduction in that of *Apiotrichum*. In contrast, in the SBR-S, both *Candida* and *Apiotrichum* steadily increased their RAs throughout the SS, SI and SII periods, cumulatively making up for > 99 % of the total abundance of fungal OTUs in SII. However, *Candida* average RA was reduced 10-fold in SIII, while the fungal community was further enriched in *Apiotrichum* (47.64 % in SII vs. 77.44 % in SIII). In addition, a reduction of the number of dominant genera was observed after the application of the DGL strategy in periods NII and SII.

Regarding the comparison between the two SBRs in each experimental period, significant differences in the RAs of the four major phyla were more often found, other than during periods NI and SI (Supplementary Table SI5). Accordingly, at the genus level, significant differences in the RAs of several dominant genera occurred between the two SBRs in each operational period (Table SI6).

The NMS biplot based on the RAs of the dominant fungal genera (Fig. 5) shows that the samples retrieved from each SBR were placed apart. This ordination confirmed that the origin of the inoculum and the NaCl concentration were major driving forces of the fungal community structure in both bioreactors, as was earlier depicted in the heatmap
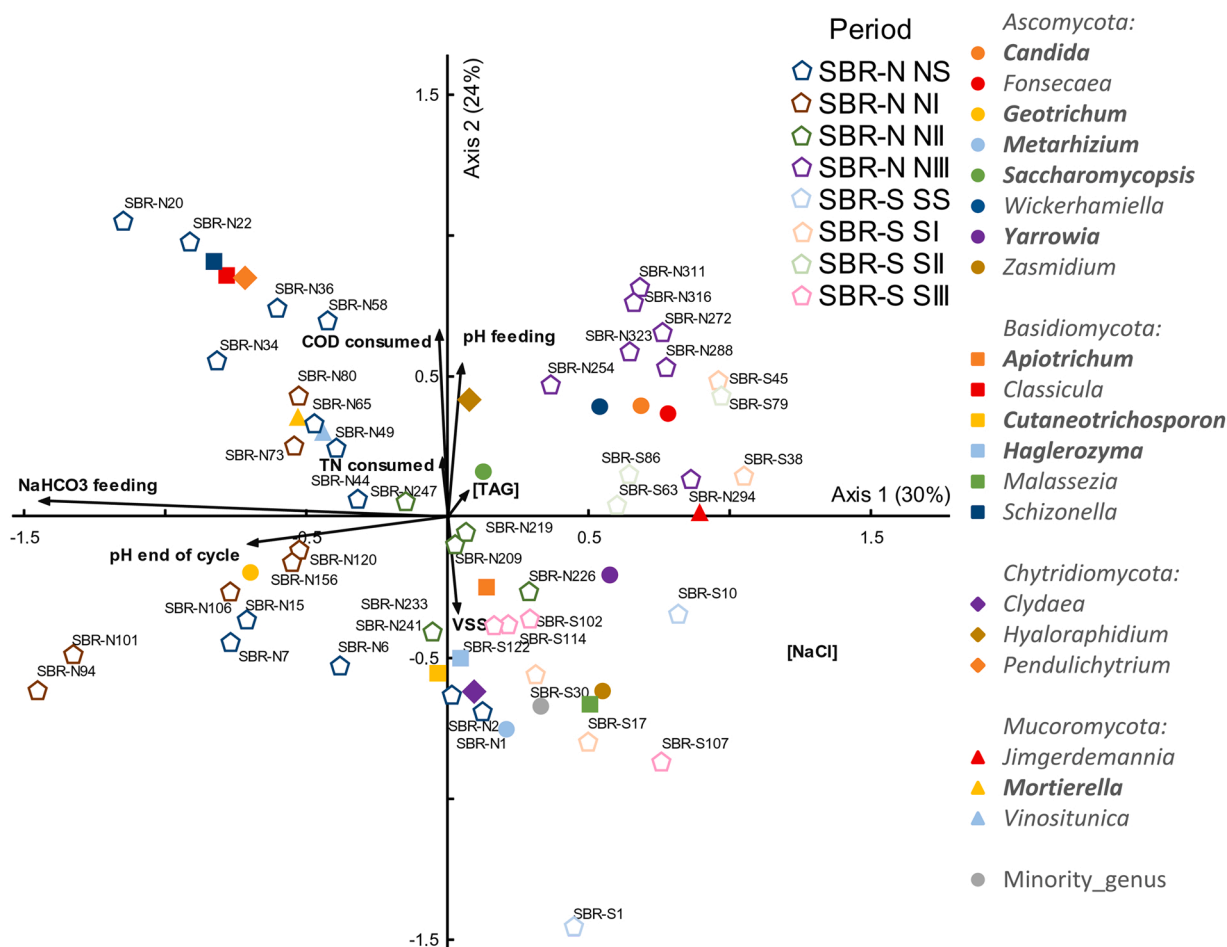

Fig. 5. Nonmetric Multidimensional Scaling (NMS) ordination of dominant fungal genera (RA > 0.5 %) from EAS (n = 2) from enrichment SBRs operated under two concentrations of NaCl (SBR-N: 0.5 g/L; SBR-S: 10 g/L), and their links with the abiotic variables influencing the EAS: NaHCO3_feeding (concentration of the NaHCO$_3$ in the feeding stream), pH_feeding (pH of the feeding stream), TN consumed (TN_consumed), VSS (volatile suspended solids concentration in the reaction medium), pH_end_of_cycle (pH at the end of the cycle), and (TAG) (intracellular TAG accumulation). The genera in boldface have been previously described as TAG accumulators.

displayed in Supplementary Fig. SI3. Several authors have earlier highlighted that the differences in NaCl concentration within the ranges applied here influenced the structure of the eukaryotic and prokaryotic communities in WWTPs [18,44]. The highest RAs of the TAG-accumulating genera *Apiotrichum* and *Yarrowia* were linked to the samples from SBR-S; hence, these salt-tolerant yeasts [45,46] could accumulate TAG under NaCl concentrations up to 10 g/L. This result is in agreement with previous studies [47,48], which concluded that the addition of NaCl at varying concentrations did not reduce the lipid accumulation performance of different fungal genera, compared with cultivation at 0 M NaCl.

The samples were sub-grouped according to the operational periods for a given SBR. Moreover, the implementation of the DGL strategy led to a narrower distribution of the samples in both SBRs (NII, NIII, SII, and SIII periods), due to a stronger selection of the fungal genera that resulted in a different community structure compared to the samples retrieved when the conventional ADF strategy was applied (NS, SS, NI, and SI periods). Thus, the enrichment strategies also modulated the fungal community structure in both SBRs. Other works have previously highlighted that the changes of operating conditions are also prime movers of the fungal community structure and diversity in engineered systems [49].

The relationships between the changes of the main operating parameters, the TAG-accumulating capacity, and the RAs of the main fungal genera revealed several strong correlations (Fig. 5, Supplementary Table SI7). The reduction of NaHCO$_3$ addition and, subsequently, the mildly acidic pH at the end of the cycle in the SBR-N, also had an important effect in the shaping of the fungal community structure (Supplementary Table SI7). The increase in the RA of *Candida* observed in NIII indicated that this well-known TAG-accumulating genus is highly responsive to changes of pH, which could be linked to the restoration of the TAG accumulation capacity. On the other hand, not enough acidification was achieved in the SBR-S during the SIII period, so this strategy did not favor *Candida*, which in fact was displaced as the dominant genus by *Apiotrichum*. Different genera of fungi previously described as TAG-accumulators dominated the community in each type of samples. However, the TAG-accumulation capacity was the variable showing the weakest relationship with the ordination of the samples based on the RAs of the dominant fungal genera, according to the small magnitude of its vector (Fig. 5). Hence, the increase of RAs of particular genera of oleaginous fungi could not be linked to a higher functionality, under any of the conditions tested.

3.5. Potential of the dominant fungal genera to contribute to TAG accumulation in the SBR

In the present study, different genera of oleaginous fungi were identified in the EAS samples. *Apiotrichum* (*Basidiomycota*) is able to synthesize TAGs from different low-cost industrial substrates [50]. This genus grows on fats and oils [51], and the *ex novo* accumulating pathway has been earlier described [52]. *Candida* (*Ascomycota*) is a promising organism for the synthesis of biodiesel precursors as it stores lipids up to 67 % of its cell dry weight using oleic acid as substrate [53]. *Cutaneotrichosporon* (*Basidiomycota*) has the ability to utilize several carbon sources and complex waste materials as feedstocks resulting in a high yield of lipid synthesis and storage [54]; however, the *ex novo* pathway has not been previously recorded in these organisms. The TAG-storage capacity of *Geotrichum* (*Ascomycota*) was described earlier [55], and its ability to use hydrophobic substrates has also been reported [8]. *Metarhizium* (*Ascomycota*) is able to synthesize TAG from glucose and potassium oleate with an accumulating capacity < 20 % of the cell dry weight [56]. The mold *Mortierella* (*Mucoromycota*) can store lipids amounting up to 50 % of its hyphal dry weight using carbohydrates and agricultural wastes [57,58]. However, TAG synthesis and accumulation using hydrophobic substrates has not been demonstrated yet for this genus. The teleomorphic yeast *Saccharomycopsis* (*Ascomycota*) can

accumulate TAG up to 50 % of the cell dry weight [59], although others [60] have described a lower TAG-accumulating capacity for this genus. The *ex novo* pathway has not been previously recorded in *Saccharomycopsis*. Finally, the dimorphic yeast *Yarrowia* is one of the best-characterized microorganisms able to accumulate lipids through the *ex novo* pathway [61], and it is widely used in single culture to produce TAG [62].

Overall, around 80 % of the total sequences retrieved from the Illumina sequencing belonged to TAG-accumulating genera, regardless of the bioreactor analyzed. Hence, the use of MMCs under the F/F regime resulted in a highly functionally organized fungal community with a substantial selection of TAG-accumulating fungi, regardless of the NaCl concentration tested and the source of inoculum. This strategy provides several advantages (relatively fast duplication rate, high metabolic activity, and ability to grow on waste substrates) that ease commercial-scale TAG production [63]. In the present study, higher levels of TAG accumulation were not correlated to the increased RA of any specific genus of fungi (Fig. 5). Nonetheless, since several well-recognized TAG-accumulating genera alternated in dominance in the SBRs' fungal community throughout operation, lack of such correlations may be linked to functional redundancy. Also it should be noted that the TAG-accumulation was < 20 wt%, thus indicating a low performance of the TAG-accumulating fungi under the operational parameters analyzed. Further research is necessary to obtain a highly functional TAG-accumulating MMC and assess the main operational parameters that stimulate the TAG accumulation capacities, in order to increase the yield of the TAG in SBRs using fish-canning oil wastes before the system scale-up.

4. Conclusions

- Fungal populations reached absolute abundances ranging from < 10^5-10^{11} 18S rRNA copies/L of EAS during steady-state operation in the SBRs using waste fish oil as a substrate for TAG accumulation, regardless of the NaCl concentration or the source of inoculum.
- Several fungal genera with the potential to synthesize and accumulate biodiesel precursors (TAG) were identified in both SBRs. Those reaching higher RAs were affiliated to the genera *Apiotrichum*, *Candida*, *Cutaneotrichosporon*, *Geotrichum*, *Haglerozyma*, *Metarhizium*, *Mortierella*, *Saccharomycopsis*, and *Yarrowia*.
- The implementation of the DGL enrichment strategy in periods NII and SII decreased the TAG-accumulation capacity of the biomass in both SBRs. However, TAG-accumulation was successfully restored by lowering the pH (average pH 5.70) in the SBR-N during the famine phase. Concomitantly, an increase of the RAs of several genera of fungi was observed, including *Candida*, widely reported in previous literature as able to synthesize and store lipids.
- The genera *Apiotrichum* and *Candida* are promising candidates for future industrial production of biodiesel precursors from fish oil wastes, since they were core populations in both SBRs.

Appendix A. Supporting information

Supplementary data associated with this article can be found in the online version at doi:10.1016/j.nbt.2022.08.001.

References

[1] Mahlia TMI, Syazmi ZAHS, Mofijur M, Abas AP, Bilad MR, Ong HC, et al. Patent landscape review on biodiesel production: technology updates. Renew Sustain Energy Rev 2020;118:109526. https://doi.org/10.1016/j.rser.2019.109526.

[2] Patel A, Karageorgou D, Rova E, Katapodis P, Rova U, Christakopoulos P, et al. An overview of potential oleaginous microorganisms and their role in biodiesel and omega-3 fatty acid-based industries. Microorganisms 2020;8:434. https://doi.org/10.3390/microorganisms8030434.

[3] Perona JJ. Biodiesel for the 21st century renewable energy economy. Energy LJ 2017;38:165.

[4] Qin L, Liu L, Zeng AP, Wei D. From low-cost substrates to single cell oils synthesized by oleaginous yeasts. Bioresour Technol 2017;245:1507–19. https://doi.org/10.1016/j.biortech.2017.05.163.

[5] Tabatabaei M, Alidadi A, Dehhaghi M, Panahi HKS, Lam SS, Nizami AS, et al. Fungi as bioreactors for biodiesel production. In: Jouzani GS, Tabatabaei M, Aghbashlo M, editors. Fungi in Fuel Biotechnology. Berlin: Springer; 2020. p. 39–67.

[6] Koivuranta K, Castillo S, Jouhten P, Ruohonen L, Penttilä M, Wiebe MG. Enhanced triacylglycerol production with genetically modified Trichosporon oleaginosus. Front Microbiol 2018;9:1337. https://doi.org/10.3389/fmicb.2018.01337.

[7] Martínez EJ, Raghavan V, González-Andrés F, Gómez X. New biofuel alternatives: integrating waste management and single cell oil production. Int J Mol Sci 2015; 16:9385–405. https://doi.org/10.3390/ijms16059385.

[8] Patel A, Matsakas L. A comparative study on de novo and ex novo lipid fermentation by oleaginous yeast using glucose and sonicated waste cooking oil. Ultrason Sonochem 2019;52:364–74. https://doi.org/10.1016/j.ultsonch.2018.12.010.

[9] Wang CW. Lipid droplet dynamics in budding yeast. Cell Mol Life Sci 2015;72:2677–95. https://doi.org/10.1007/s00018-015-1903-5.

[10] Dourou M, Aggeli D, Papanikolaou S, Aggelis G. Critical steps in carbon metabolism affecting lipid accumulation and their regulation in oleaginous microorganisms. Appl Microbiol Biotechnol 2018;102:2509–23. https://doi.org/10.1007/s00253-018-8813-z.

[11] Ochsenreither K, Glück C, Stressler T, Fischer L, Syldatk C. Production strategies and applications of microbial single cell oils. Front Microbiol 2016;7:1539. https://doi.org/10.3389/fmicb.2016.01539.

[12] Costa JF, Almeida MF, Alvim-Ferraz MCM, Dias JM. Biodiesel production using oil from fish canning industry wastes. Energy Convers Manag 2013;74:17–23. https://doi.org/10.1016/j.enconman.2013.04.032.

[13] da Silva TL, Santos AR, Gomes R, Reis A. Valorizing fish canning industry by-products to produce ω-3 compounds and biodiesel. Environ Technol Innov 2018;9:74–81. https://doi.org/10.1016/j.eti.2017.11.002.

[14] Tamis J, Sorokin DY, Jiang Y, van Loosdrecht MC, Kleerebezem R. Lipid recovery from a vegetable oil emulsion using microbial enrichment cultures. Biotechnol Biofuels 2015;8:1–11. https://doi.org/10.1186/s13068-015-0228-9.

[15] Lam MK, Lee KT, Mohamed AR. Homogeneous, heterogeneous and enzymatic catalysis for transesterification of high free fatty acid oil (waste cooking oil) to biodiesel: a review. Biotechnol Adv 2010;28:500–18. https://doi.org/10.1016/j.biotechadv.2010.03.002.

[16] Chopra J, Dineshkumar R, Bhaumik M, Dhanarajan G, Kumar R, Sen R. Integrated in situ transesterification for improved biodiesel production from oleaginous yeast: a value proposition for possible industrial implication. RSC Adv 2016;6:70364–73. https://doi.org/10.1039/C6RA14003C.

[17] Singh S, Pandey D, Saravanabhupathy S, Daverey A, Dutta K, Arunachalam K. Liquid wastes as a renewable feedstock for yeast biodiesel production: opportunities and challenges. Environ Res 2022;207:112100. https://doi.org/10.1016/j.envres.2021.112100.

[18] Correa-Galeote D, Roibás A, Mosquera-Corral A, Juárez-Jiménez B, González-López J, Rodelas B. Salinity is the major driver of the global eukaryotic community structure in fish-canning wastewater treatment plants. J Environ Manag 2021;290:112623. https://doi.org/10.1016/j.jenvman.2021.112623.

[19] Correa-Galeote D, Roibás A, Mosquera-Corral A, Juárez-Jiménez B, González-López J, Rodelas B. Revealing the dissimilar structure of microbial communities in different WWTPs that treat fish-canning wastewater with different NaCl content. J Water Process Eng 2021;44:102328. https://doi.org/10.1016/j.jwpe.2021.102328.

[20] Argiz L, González-Cabaleiro R, Correa-Galeote D, Val del Río Á, Mosquera-Corral A. Open-culture biotechnological process for triacylglycerides and polyhydroxyalkanoates recovery from industrial waste fish oil under saline conditions. Sep Purif Technol 2021;270:118805. https://doi.org/10.1016/j.seppur.2021.118805.

[21] Argiz L, González-Cabaleiro R, Val del Río Á, González-López J, Mosquera-Corral A. A novel strategy for triacylglycerides and polyhydroxyalkanoates production using waste lipids. Sci Total Environ 2021;763:142944. https://doi.org/10.1016/j.scitotenv.2020.142944.

[22] Walker GM, White NA. Introduction to fungal physiology. In: Kavanagh K, editor. Fungi: Biology and Applications. Hoboken: John Wiley & Sons Inc; 2018. p. 1–35.

[23] APHA. Standard methods for the examination of water and wastewater. twentyfirst ed. Washington: American Public Health Association; 2005.

[24] Smolders GJF, Van der Meij J, Van Loosdrecht MCM, Heijnen JJ. Stoichiometric model of the aerobic metabolism of the biological phosphorus removal process. Biotechnol Bioeng 1994;44:837–48. https://doi.org/10.1002/bit.260440709.

[25] Liu CM, Kachur S, Dwan MG, Abraham AG, Aziz M, Hsueh PR, et al. FungiQuant: a broad-coverage fungal quantitative real-time PCR assay. BMC Microbiol 2012;12:1–11. https://doi.org/10.1186/1471-2180-12-255.

[26] Maza-Márquez P, Castellano-Hinojosa A, González-Martínez A, Juárez-Jiménez B, González-López J, Rodelas B. Abundance of total and metabolically active Candidatus Microthrix and fungal populations in three full-scale wastewater treatment plants. Chemosphere 2019;32:26–34. https://doi.org/10.1016/j.chemosphere.2019.05.149.

[27] Schloss PD, Westcott SL, Ryabin T, Hall JR, Hartmann M, Hollister EB, et al. Introducing Mothur: open-source, platform-independent, community-supported software for describing and comparing microbial communities. Appl Environ Microbiol 2009;75:7537–41. https://doi.org/10.1128/AEM.01541-09.

[28] Hill TC, Walsh KA, Harris JA, Moffett BF. Using ecological diversity measures with bacterial communities. FEMS Microbiol Ecol 2003;43:1–11. https://doi.org/10.1111/j.1574-6941.2003.tb01040.x.

[29] Wei Z, Liu Y, Feng K, Li S, Wang S, Jin D, et al. The divergence between fungal and bacterial communities in seasonal and spatial variations of wastewater treatment plants. Sci Total Environ 2018;628:969–78. https://doi.org/10.1016/j.scitotenv.2018.02.003.

[30] Corsino SF, Di Trapani D, Torregrossa M, Viviani G. Aerobic granular sludge treating high strength citrus wastewater: analysis of pH and organic loading rate effect on kinetics, performance and stability. J Environ Manag 2018;214:23–35. https://doi.org/10.1016/j.jenvman.2018.02.087.

[31] Zhang DM, Teng Q, Zhang D, Jilani G, Ken WM, Yang ZP, et al. Performance and microbial community dynamics in anaerobic continuously stirred tank reactor and sequencing batch reactor (CSTR-SBR) coupled with magnesium-ammonium-phosphate (MAP)-precipitation for treating swine wastewater. Bioresour Technol 2021;320:124336. https://doi.org/10.1016/j.biortech.2020.124336.

[32] Yao J, Liu J, Zhang Y, Xu S, Hong Y, Chen Y. Adding an anaerobic step can rapidly inhibit sludge bulking in SBR reactor. Sci Rep 2019;9:1–10. https://doi.org/10.1038/s41598-019-47304-3.

[33] Cortés-Lorenzo C, González-Martínez A, Smidt H, González-López J, Rodelas B. Influence of salinity on fungal communities in a submerged fixed bed bioreactor for wastewater treatment. Chem Eng J 2016;285:562–72. https://doi.org/10.1016/j.cej.2015.10.009.

[34] Maza-Márquez P, Vilchez-Vargas R, Kerckhof FM, Aranda E, González-López J, Rodelas B. Community structure, population dynamics and diversity of fungi in a full-scale membrane bioreactor (MBR) for urban wastewater treatment. Water Res 2016;105:507–19.

[35] Niu L, Li Y, Xu L, Wang P, Zhang W, Wang C, et al. Ignored fungal community in activated sludge wastewater treatment plants: diversity and altitudinal characteristics. Environ Sci Pollut Res 2017;24:4185–93. https://doi.org/10.1016/j.watres.2016.09.021.

[36] Fortela DL, Hernandez R, Chistoserdov A, Zappi M, Bajpai R, Gang D, et al. Biodiesel profile stabilization and microbial community selection of activated sludge feeding on acetic acid as a carbon source. ACS Sustain Chem Eng 2016;4:6427–34. https://doi.org/10.1021/acssuschemeng.6b01140.

[37] Assress HA, Selvarajan R, Nyoni H, Ntushelo K, Mamba BB, Msagati TA. Diversity, co-occurrence and implications of fungal communities in wastewater treatment plants. Sci Rep 2019;9:1–15. https://doi.org/10.1038/s41598-019-50624-z.

[38] Navrozidou E, Remmas N, Melidis P, Karpouzas DG, Tsiamis G, Ntougias S. Biodegradation potential and diversity of diclofenac-degrading microbiota in an immobilized cell biofilter. Processes 2019;7:554. https://doi.org/10.3390/pr7090554.

[39] Qu H, Meng N, Liu S, Wang J, Sun Y, Ma Q. Bacterial and fungal community compositions and structures of a skatole-degrading culture enriched from pig slurry. 3 Biotech 2020;10:1–4. https://doi.org/10.1007/s13205-020-02465-1.

[40] Zhang S, Fan F, Meng F. Seasonality and community separation of fungi in a municipal wastewater treatment plant. Appl Environ Microbiol 2020;86:e00991–20. https://doi.org/10.1128/AEM.00991-20.

[41] Qian X, Li H, Wang Y, Wu B, Wu M, Chen L, et al. Leaf and root endospheres harbor lower fungal diversity and less complex fungal co-occurrence patterns than rhizosphere. Front Microbiol 2019;10:1015. https://doi.org/10.3389/fmicb.2019.01015.

[42] Assress HA, Selvarajan R, Nyoni H, Ogola HJO, Mamba BB, Msagati TA. Azole antifungal resistance in fungal isolates from wastewater treatment plant effluents. Environ Sci Pollut Res 2021;28:3217–29. https://doi.org/10.1007/s11356-020-10688-1.

[43] Zhang P, Shen Y, Guo JS, Li C, Wang H, Chen YP, et al. Extracellular protein analysis of activated sludge and their functions in wastewater treatment plant by shotgun proteomics. Sci Rep 2015;5:1–11. https://doi.org/10.1038/srep12041.

[44] Rodriguez-Sanchez A, Leyva-Diaz JC, Muñoz-Palazon B, Poyatos JM, Gonzalez-Lopez J. Influence of salinity cycles in bioreactor performance and microbial community structure of membrane-based tidal-like variable salinity wastewater treatment systems. Environ Sci Pollut Res 2019;26:514–27. https://doi.org/10.1007/s11356-018-3608-4.

[45] Bankar AV, Kumar AR, Zinjarde SS. Environmental and industrial applications of Yarrowia lipolytica. Appl Microbiol Biotechnol 2009;84:847–65. https://doi.org/10.1007/s00253-009-2156-8.

[46] James SA, Bond CJ, Stanley R, Ravella SR, Péter G, Dlauchy D, et al. Apiotrichum terrigenum sp. nov.; a soil-associated yeast found in both the UK and mainland Europe. Int J Syst Evol Microbiol 2016;66:5046. https://doi.org/10.1099/ijsem.0.001467.

[47] Subhash GV, Mohan SV. Lipid accumulation for biodiesel production by oleaginous fungus Aspergillus awamori: influence of critical factors. Fuel 2014;116:509–15. https://doi.org/10.1016/j.fuel.2013.08.035.

[48] Tchakouteu SS, Kopsahelis N, Chatzifragkou A, Kalantzi O, Stoforos NG, Koutinas AA, et al. Rhodosporidium toruloides cultivated in NaCl-enriched

glucose-based media: adaptation dynamics and lipid production. Eng Life Sci 2017; 17:237–48. https://doi.org/10.1002/elsc.201500125.

[49] Badia-Fabregat M, Lucas D, Tuomivirta T, Fritze H, Pennanen T, Rodríguez-Mozaz S, et al. Study of the effect of the bacterial and fungal communities present in real wastewater effluents on the performance of fungal treatments. Sci Total Environ 2017;579:366–77. https://doi.org/10.1016/j.scitotenv.2016.11.088.

[50] Qian X, Zhou X, Chen L, Zhang X, Xin F, Dong W, et al. Bioconversion of volatile fatty acids into lipids by the oleaginous yeast Apiotrichum porosum DSM27194. Fuel 2021;290:119811. https://doi.org/10.1016/j.fuel.2020.119811.

[51] Athenaki M, Gardeli C, Diamantopoulou P, Tchakouteu SS, Sarris D, Philippoussis A, et al. Lipids from yeasts and fungi: physiology, production and analytical considerations. J Appl Microbiol 2018;124:336–67. https://doi.org/10.1111/jam.13633.

[52] Lee I, Hammond EG, Cornette JL, Glatz BA. Triacylglycerol assembly from binary mixtures of fatty acids by Apiotrichum curvatum. Lipids 1993;28:1055–61. https://doi.org/10.1007/BF02537070.

[53] Morin N, Czerwiec Q, Nicaud JM, Neuvéglise C, Rossignol T. Transforming Candida hispaniensis, a promising oleaginous and flavogenic yeast. Yeast 2020;37: 348–55. https://doi.org/10.1002/yea.3466.

[54] Awad D, Bohnen F, Mehlmer N, Brueck T. Multi-factorial-guided media optimization for enhanced biomass and lipid formation by the oleaginous yeast Cutaneotrichosporon oleaginosus. Front Bioeng Biotechnol 2019;7:54. https://doi.org/10.3389/fbioe.2019.00054.

[55] Liu LP, Zong MH, Linhardt RJ, Lou WY, Li N, Huang C, et al. Mechanistic insights into the effect of imidazolium ionic liquid on lipid production by Geotrichum

fermentans. Biotechnol Biofuels 2016;9:1–13. https://doi.org/10.1186/s13068-016-0682-z.

[56] Stolarek P, Różalska S, Bernat P. Lipidomic adaptations of the Metarhizium robertsii strain in response to the presence of butyltin compounds. Biochim Biophys Acta Biomembr 2019;1861:316–26. https://doi.org/10.1016/j.bbamem.2018.06.007.

[57] Wang H, Zhang C, Chen H, Gu Z, Zhao J, Zhang H, et al. Tetrahydrobiopterin plays a functionally significant role in lipogenesis in the oleaginous fungus Mortierella alpina. Front Microbiol 2020;11:250. https://doi.org/10.3389/fmicb.2020.00250.

[58] Xing D, Wang H, Pan A, Wang J, Xue D. Assimilation of corn fiber hydrolysates and lipid accumulation by Mortierella isabellina. Biomass– Bioenergy 2012;39: 494–501. https://doi.org/10.1016/j.biombioe.2012.01.024.

[59] Sebolai OM. The lipid composition of the yeast genus Saccharomycopsis. South Africa: Bloemfontein: Doctoral Thesis University of the Free State; 2004.

[60] Kanti A, Sudiana IM. Co-culture of amylolytic fungi Aspergillus niger and oleaginous yeast Candida orthopsilosis on cassava waste for lipid accumulation. Ber Biol 2017;16:111–9. https://doi.org/10.14203/beritabiologi.v16i2.2207.

[61] Kieliszek M, Dourou M. Effect of selenium on the growth and lipid accumulation of Yarrowia lipolytica yeast. Biol Trace Elem Res 2021;199:1611–22. https://doi.org/10.1007/s12011-020-02266-w.

[62] Wang J, Ledesma-Amaro R, Wei Y, Ji B, Ji XJ. Metabolic engineering for increased lipid accumulation in Yarrowia lipolytica - a review. Bioresour Technol 2020;313: 123707. https://doi.org/10.1016/j.biortech.2020.123707.

[63] Diwan B, Gupta P. A Deuteromycete isolate Geotrichum candidum as oleaginous cell factory for medium-chain fatty acid-rich oils. Curr Microbiol 2020;77: 3738–49. https://doi.org/10.1007/s00284-020-02155-4.